Available online at www.sciencedirect.com

SCIENCE DIRECT®

International Journal of Heat and Mass Transfer 49 (2006) 1986–1990

International Journal of HEAT and MASS TRANSFER

www.elsevier.com/locate/ijhmt

Technical Note

Effect of rounded corners on the secondary flow of viscoelastic fluids through non-circular ducts

S.H. Hashemabadi [a,1], S.Gh. Etemad [b,*]

[a] Department of Chemical Engineering, Iran University of Science and Technology, Narmak, Tehran, Iran
[b] Department of Chemical Engineering, Isfahan University of Technology, Isfahan, Iran

Received 14 March 2005; received in revised form 14 November 2005

Abstract

The Reiner–Rivlin viscoelastic model was used to investigate numerically on the pattern and strength of the secondary flows in rounded corners square ducts. The influence of rheological properties on flow domain was studied. The governing equations for steady state, laminar fully developed flow were solved by finite difference method. It is shown the secondary flow of a Reiner–Rivlin fluid has a negligible effect on the axial flow and $f \cdot Re$. Viscous and elastic behaviors as well as the rounding of the corners have important effects on the secondary flows created by viscoelastic fluid.

Keywords: Secondary flow; Viscoelastic; Non-circular ducts; Numerical solution; Reiner–Rivlin

1. Introduction

Investigation about the viscoelastic fluid flow becomes increasingly important due to wide range of application of such fluids in many industries such as polymer processing. Viscoelastic fluid flow through noncircular channels under laminar condition causes the presence of secondary flows, which is due to the fact that the stresses acting on orthogonal faces of a fluid element are not equal [1]. The existence of such secondary flows was also obtained by numerical simulation using the Criminale–Ericksen–Fibley (CEF) model [2–5], Reiner–Rivlin model [6] and Phan–Thien–Tanner (PTT) model [7]. Dodsen et al. [8] used CEF fluid model and solved governing equations by perturbation method where the solution expanded in powers of second normal stress coefficient ψ_2. Based on their results the effect of the secondary flows on pressure drop is small at low flow rates which increases at higher flow rates. Generally, for different aspect ratios, there are two vortices in each quadrant of the rectangular duct. The vortices are very sensitive to the viscous and elastic effects of viscoelastic fluid.

The effect of rectangular duct aspect ratio on secondary flow of viscoelastic fluid has been reported by several researchers. But the effect of sharp corners of rectangular channel on pattern and strength of secondary flow of viscoelastic fluid has not been reported. The aim of present study is to investigate numerically on the laminar flow of Reiner–Rivlin viscoelastic fluid through square duct with different rounding of corners.

2. Mathematical formulation

Fig. 1 shows a schematic diagram of the system under consideration. Constant property, fully developed and laminar flow of Reiner–Rivlin viscoelastic fluid model are considered. The governing equation can be expressed as follows [9]:

Continuity equation:

$$\frac{\partial u}{\partial x} + \frac{\partial v}{\partial y} = 0. \quad (1)$$

* Corresponding author. Tel.: +98 311 3915625; fax: +98 311 3912677.
E-mail address: etemad@cc.iut.ac.ir (S.Gh. Etemad).
1 Tel.: +98 21 7391 2714; fax: +98 21 7724 0495.

0017-9310/$ - see front matter © 2006 Elsevier Ltd. All rights reserved.
doi:10.1016/j.ijheatmasstransfer.2006.01.014

Nomenclature

D_h	duct hydraulic diameter
f	fanning friction factor
K	consistency index
n	power law index
p	pressure
r	radius of corner (refer to Fig. 1)
Re_g	generalized Reynolds number, $\frac{\rho D_h^n \bar{w}^{2-n}}{K}$
S	dimensionless transverse velocity
u, v, w	velocity components in x, y, and z
x, y, z	cartesian coordinates

Greek symbols

ϕ	stream function
η	apparent viscosity
$\dot{\gamma}$	rate of deformation tensor
$\boldsymbol{v}$	velocity vector
ρ	density
$\boldsymbol{\tau}$	stress tensor
ψ_2	second normal stress coefficient

Subscripts

g	generalized
max	maximum value
mean	mean value
w	value at wall

Superscript

*	dimensionless value

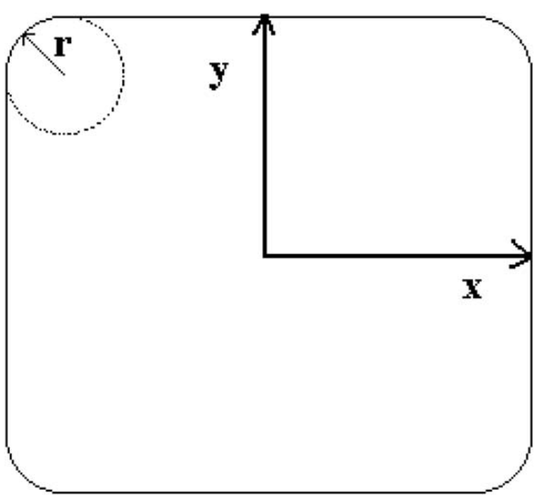

Fig. 1. Schematic of flow domain.

Momentum equations:

$$\rho\left(u\frac{\partial u}{\partial x}+v\frac{\partial u}{\partial y}\right)=-\frac{\partial p}{\partial x}-\left[\frac{\partial \tau_{yx}}{\partial y}+\frac{\partial \tau_{xx}}{\partial x}\right], \quad (2)$$

$$\rho\left(u\frac{\partial v}{\partial x}+v\frac{\partial v}{\partial y}\right)=-\frac{\partial p}{\partial y}-\left[\frac{\partial \tau_{xy}}{\partial x}+\frac{\partial \tau_{yy}}{\partial y}\right], \quad (3)$$

$$\rho\left(u\frac{\partial w}{\partial x}+v\frac{\partial w}{\partial y}\right)=-\frac{\partial p}{\partial z}-\left[\frac{\partial \tau_{xz}}{\partial x}+\frac{\partial \tau_{yz}}{\partial y}\right]. \quad (4)$$

The Eqs. (1)–(4) with no slip boundary condition at walls are solved to predict the secondary flow of Reiner–Rivlin viscoelastic fluid model in the square channel. The Reiner–Rivlin viscoelastic fluid model can be defined as follows [9]:

$$\boldsymbol{\tau}=-\eta\dot{\gamma}-\psi_2\dot{\gamma}\cdot\dot{\gamma}, \quad (5)$$

where ψ_2 is second normal stress difference coefficient and $\dot{\gamma}$ is given as

$$\dot{\gamma}=\begin{pmatrix} 2\frac{\partial u}{\partial x} & \frac{\partial v}{\partial x}+\frac{\partial u}{\partial y} & \frac{\partial w}{\partial x} \\ \frac{\partial v}{\partial x}+\frac{\partial u}{\partial y} & 2\frac{\partial v}{\partial y} & \frac{\partial w}{\partial y} \\ \frac{\partial w}{\partial x} & \frac{\partial w}{\partial y} & 0 \end{pmatrix}. \quad (6)$$

Substitution of rate of deformation tensor, after performing an order of magnitude analysis on Eq. (5), stress tensor component can be obtained as following equations:

$$\tau_{xx}=-2\eta\left(\frac{\partial u}{\partial x}\right)-\psi_2\left(\frac{\partial w}{\partial x}\right)^2, \quad (7)$$

$$\tau_{xy}=-\eta\left(\frac{\partial u}{\partial y}+\frac{\partial v}{\partial x}\right)-\psi_2\frac{\partial w}{\partial x}\frac{\partial w}{\partial y}, \quad (8)$$

$$\tau_{yy}=-2\eta\left(\frac{\partial v}{\partial y}\right)-\psi_2\left(\frac{\partial w}{\partial y}\right)^2, \quad (9)$$

$$\tau_{xz}=-\eta\frac{\partial w}{\partial x}-\psi_2\left[\frac{\partial w}{\partial y}\left(\frac{\partial u}{\partial y}+\frac{\partial v}{\partial x}\right)+2\frac{\partial u}{\partial x}\frac{\partial w}{\partial x}\right], \quad (10)$$

$$\tau_{yz}=-\eta\frac{\partial w}{\partial y}-\psi_2\left[\frac{\partial w}{\partial x}\left(\frac{\partial u}{\partial y}+\frac{\partial v}{\partial x}\right)+2\frac{\partial v}{\partial y}\frac{\partial w}{\partial y}\right], \quad (11)$$

where η is the apparent viscosity for generalized non-Newtonian model which can be calculated from power law viscosity model

$$\eta=K\dot{\gamma}^{n-1} \quad (12)$$

The stream function approach is one of the popular methods for solving the 2-D incompressible motion equations. In this approach, the stream function ϕ is defined by the following equations:

$$u=-\frac{\partial\phi}{\partial y},\quad v=\frac{\partial\phi}{\partial x}. \quad (13)$$

Using the new dependent variable and Eqs. (7)–(9), the two momentum Eqs. (2) and (3) can be combined (thereby eliminating pressure) to give

$$\frac{\partial^4\phi^*}{\partial x^{*4}}+2\frac{\partial^4\phi^*}{\partial x^{*2}\partial y^{*2}}+\frac{\partial^4\phi^*}{\partial y^{*4}}=F1, \tag{14}$$

where

$$\begin{aligned}
F1&=\eta^{*^{-1}}\left[\psi_2^*F1_1+Re_gF1_2+F1_3\right],\\
F1_1&=\frac{\partial w^*}{\partial x^*}\frac{\partial}{\partial y^*}\left(\frac{\partial^2 w^*}{\partial x^{*2}}+\frac{\partial^2 w^*}{\partial y^{*2}}\right)-\frac{\partial w^*}{\partial y^*}\frac{\partial}{\partial x^*}\left(\frac{\partial^2 w^*}{\partial x^{*2}}+\frac{\partial^2 w^*}{\partial y^{*2}}\right),\\
F1_2&=\frac{\partial\phi}{\partial x^*}\frac{\partial F1_4}{\partial y^*}-\frac{\partial\phi}{\partial y^*}\frac{\partial F1_4}{\partial x^*},\\
F1_3&=\left(\frac{\partial^2\eta^*}{\partial y^{*2}}-\frac{\partial^2\eta^*}{\partial x^{*2}}\right)\left(\frac{\partial^2\phi^*}{\partial x^{*2}}-\frac{\partial^2\phi^*}{\partial y^{*2}}\right)-4\frac{\partial^2\eta^*}{\partial x^*\partial y^*}\frac{\partial^2\phi^*}{\partial x^*\partial y^*}\\
&\quad-2\left(\frac{\partial\eta^*}{\partial x^*}\frac{\partial F1_4}{\partial x^*}+\frac{\partial\eta^*}{\partial y^*}\frac{\partial F1_4}{\partial y^*}\right),\\
F1_4&=\frac{\partial^2\phi^*}{\partial x^{*2}}+\frac{\partial^2\phi^*}{\partial y^{*2}}.
\end{aligned} \tag{15}$$

The dimensionless z-momentum equation is

$$\frac{\partial}{\partial x^*}\left(\eta^*\frac{\partial w^*}{\partial x^*}\right)+\frac{\partial}{\partial y^*}\left(\eta^*\frac{\partial w^*}{\partial y^*}\right)=F2, \tag{16}$$

where right hand side of Eq. (14) is as follows:

$$\begin{aligned}
F2&=-2fRe_g+Re_gF2_1+\psi_2^*(F2_2-F2_3),\\
F2_1&=\frac{\partial\phi^*}{\partial x^*}\frac{\partial w^*}{\partial y^*}-\frac{\partial\phi^*}{\partial y^*}\frac{\partial w^*}{\partial x^*},\\
F2_2&=\frac{\partial w^*}{\partial x^*}\frac{\partial}{\partial y^*}\left(\frac{\partial^2\phi^*}{\partial x^{*2}}+\frac{\partial^2\phi^*}{\partial y^{*2}}\right)-\frac{\partial w^*}{\partial y^*}\frac{\partial}{\partial x^*}\left(\frac{\partial^2\phi^*}{\partial x^{*2}}+\frac{\partial^2\phi^*}{\partial y^{*2}}\right),\\
F2_3&=2\left[\frac{\partial^2\phi^*}{\partial x^*\partial y^*}\left(\frac{\partial^2 w^*}{\partial y^{*2}}-\frac{\partial^2 w^*}{\partial x^{*2}}\right)+\frac{\partial^2 w^*}{\partial x^*\partial y^*}\left(\frac{\partial^2\phi^*}{\partial x^{*2}}-\frac{\partial^2\phi^*}{\partial y^{*2}}\right)\right].
\end{aligned} \tag{17}$$

The dimensionless apparent viscosity η^* can be written

$$\eta^*=\dot\gamma^{*^{n-1}}, \tag{18}$$

where dimensionless magnitude of $\dot\gamma^*$ can be calculated as follows:

$$\dot\gamma^*=\sqrt{\frac{1}{2}\sum_i\sum_j\dot\gamma_{ij}^*\dot\gamma_{ji}^*} \tag{19}$$

Therefore,

$$\eta^*=\left[\left(\frac{\partial w^*}{\partial x^*}\right)^2+\left(\frac{\partial w^*}{\partial y^*}\right)^2+4\left(\frac{\partial^2\phi}{\partial x^*\partial y^*}\right)^2+\left(\frac{\partial^2\phi}{\partial x^{*2}}-\frac{\partial^2\phi}{\partial y^{*2}}\right)^2+c_0\right]^{\frac{n-1}{2}}. \tag{20}$$

The dimensionless variables are defined as

$$x^*=\frac{x}{D_h},\quad y^*=\frac{y}{D_h},\quad z^*=\frac{z}{D_h},\quad w^*=\frac{w}{\bar w},$$
$$\psi_2^*=\frac{\bar w^{2-n}\psi_2}{\eta D_h^{2-n}},\quad \phi^*=\frac{\phi}{\bar w D_h},\quad \eta^*=\frac{\eta}{K}\left(\frac{\bar w}{D_h}\right)^{1-n}.$$

The Fanning friction factor and generalized Reynolds number are defined as follows:

$$f=\frac{\tau_w}{\frac{1}{2}\rho\bar w^2}=-\frac{D_h}{2\rho\bar w^2}\frac{dp}{dz}, \tag{21}$$

$$Re_g=\frac{\rho D_h^n\bar w^{2-n}}{K}. \tag{22}$$

The dimensionless boundary conditions are

$$\begin{aligned}w^*(x^*,0.5)&=w^*(x^*,-0.5)=w^*(0.5,y^*)\\&=w^*(-0.5,y^*)=0,\end{aligned} \tag{23}$$

$$\begin{aligned}\phi^*(x^*,0.5)&=\phi^*(x^*,-0.5)=\phi^*(0.5,y^*)\\&=\phi^*(-0.5,y^*)=0.\end{aligned} \tag{24}$$

3. Solution and results

Eqs. (14) and (16), with the appropriate boundary conditions (23) and (24), are solved numerically employing the finite difference technique. In this study very fine meshes are used to cover all edges of duct and circular arc in corners. Table 1 illustrates the calculated product of friction factor and Reynolds number fRe_g error obtained with different meshes for Newtonian fluid by this study and exact solution available in the literature. The exact solution result of fRe_g for Newtonian fluid flow through square duct is 14.2 [10] and the relative difference of the results of this investigation and exact solution for 200×200 mesh number is 0.8%. Therefore, the number of meshes based on mesh independency of variables (200×200) is used for all simulations. Further refining of meshes does not change the value of the results.

The calculated fRe_g in this work for power law model ($\psi_2^*=0$) shows good agreement with other available results in the literature Table 2. Based on the results the influence of the secondary flows on the axial velocity profile w^*, is negligible even in corners that the vortices are expected.

ψ_2^* and power law index n, have considerable effects on the production of friction factor and Reynolds number Fig. 2 but for $n=1$ the effect of ψ_2^* is negligible.

In order of evaluate of secondary flows strength, the mean and maximum transverse velocities, are defined as follows:

$$S_{mean}=\int_{-0.5}^{0.5}\int_{-0.5}^{0.5}\sqrt{u^{*2}+v^{*2}}\,dx\,dy,$$
$$S_{max}=\mathrm{Max}\left(\sqrt{u^{*2}+v^{*2}}\right) \tag{25}$$

Table 1
Grid independency for Newtonian fluid—relative error between the results of this study and exact solution [10]

Grid	20×20	40×40	60×60	80×80	100×100	200×200
% Error	6.4	3.9	2.7	2.1	1.7	0.8

Table 2
Comparision of fRe_g obtained by this investigation and available results in the literature

fRe_g n	Square ($r = 0$)			$r = 0.2$	$r = 0.4$	Pipe ($r = 0.5$)	
	Kozicki	Wheeler	Present	Present	Present	Kozicki	Present
0.5	5.935	5. 723	5.674	5.655	5.888	6.325	6.248
0.6	7.089	6.883	6.811	6.785	7.072	7.639	7.530
0.7	8.451	8.268	8.165	8.124	8.477	9.207	9.055
0.8	10.061	9.915	9.778	9.716	10.147	11.081	10.873
0.9	11.965	11.905	11.685	11.608	12.132	13.321	13.043
1.0	14.219	14.228	14.09	13.860	14.494	16.000	15.753

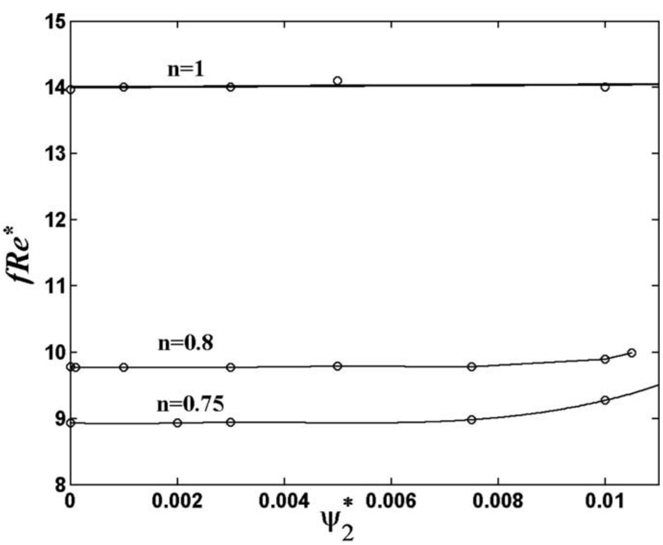

Fig. 2. The effect of ψ_2^* on fRe_g ($r = 0$, $Re_g = 500$).

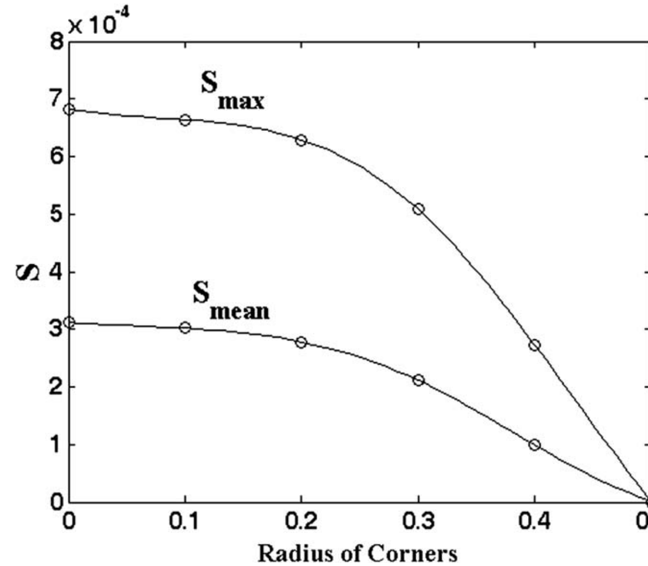

Fig. 3. The effect of roundness on strength of secondary flows ($\psi_2^* = 0.005$, $n = 0.8$, $Re_g = 500$).

Table 3
The effect of roundness of corners on secondary flows ($n = 0.8$, $Re_g = 500$, $\psi_2^* = 0.01$)

r	ϕ_{min}	ϕ_{max}	S_{max}	S_{mean}
0	-4.72×10^{-4}	4.72×10^{-4}	5.93×10^{-3}	2.53×10^{-3}
0.1	-3.65×10^{-4}	3.65×10^{-4}	4.51×10^{-3}	1.97×10^{-3}
0.2	-3.02×10^{-4}	3.02×10^{-4}	3.71×10^{-3}	1.62×10^{-3}
0.3	-1.39×10^{-4}	1.39×10^{-4}	1.86×10^{-3}	6.95×10^{-4}
0.4	-7.78×10^{-5}	7.78×10^{-5}	1.03×10^{-3}	3.90×10^{-4}
0.5	-1.29×10^{-6}	1.29×10^{-6}	6.73×10^{-5}	5.90×10^{-6}

Based on the results for each channel two same size and same strength vortices are appeared at each quadrant. Increasing the roundness of the corners causes the weaker vortices which in limiting case for round tube these vortices are negligible Table 3.

Figs. 3 and 4 show the effects of roundness of corners on secondary flow for $\psi_2^* = 0.005$ and $\psi_2^* = 0.01$, respectively. From the results of these figures a greater second normal stress coefficient has strong effect on dimensionless transverse velocity. The influences of the roundness of corners on transverse velocity vector and stream function contour are demonstrated in Figs. 5 and 6. Based on the results decreasing of roundness enhances the strength of secondary flow in channel, for example for rounded square duct with $r = 0.3$ the maximum of stream function, $\phi_{max} = 1.388 \times 10^{-4}$, will be about 3.4 times less than that for square duct ($r = 0$), $\phi_{max} = 4.723 \times 10^{-4}$.

4. Conclusion

The secondary flows of Reiner–Rivlin viscoelastic fluid model in laminar fully developed flow through rounded corners square duct were studied numerically.

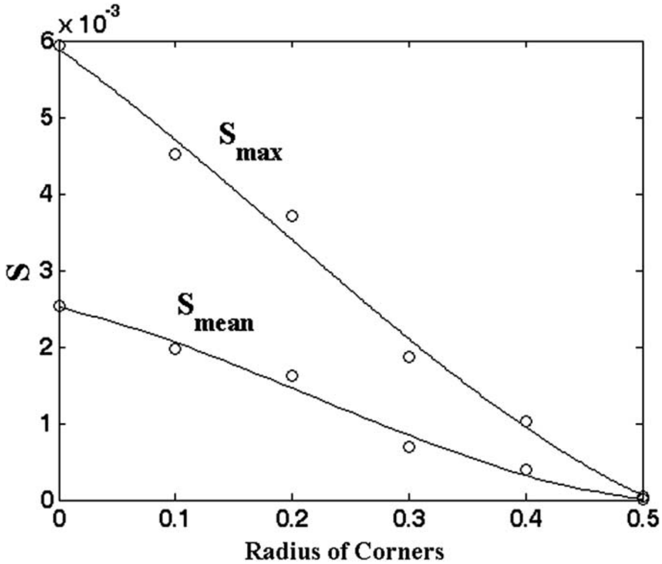

Fig. 4. The effect of roundness on strength of secondary flows ($\psi_2^* = 0.01$, $n = 0.8$, $Re_g = 500$).

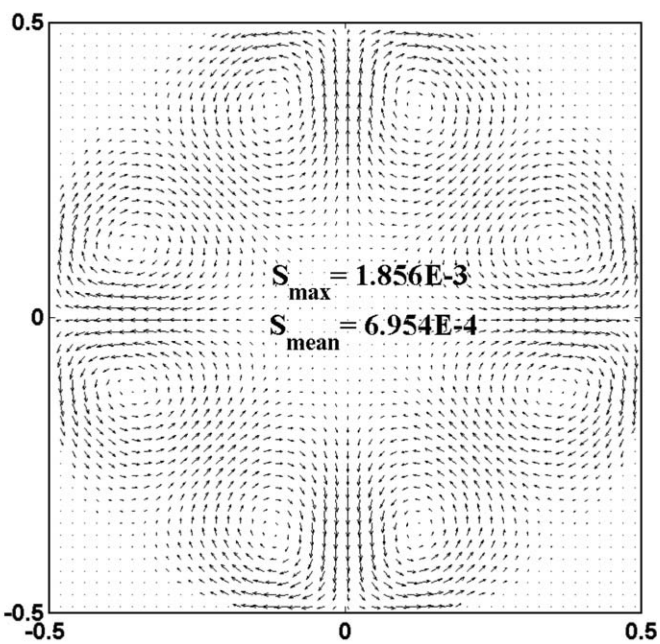

Fig. 5. Transverse velocity vector ($n = 0.8$, $Re_g = 500$, $\psi_2^* = 0.01$, $r = 0.3$).

Four different roundness (0.1–0.4) were considered with a wide range of second normal stress coefficients. Based on the numerical results the effect of elasticity on axial velocity and production of friction factor and Reynolds number is negligible. The general pattern of secondary flows in the square duct with rounded corners are similar to that of the channel with sharp corners. Rounding corners causes

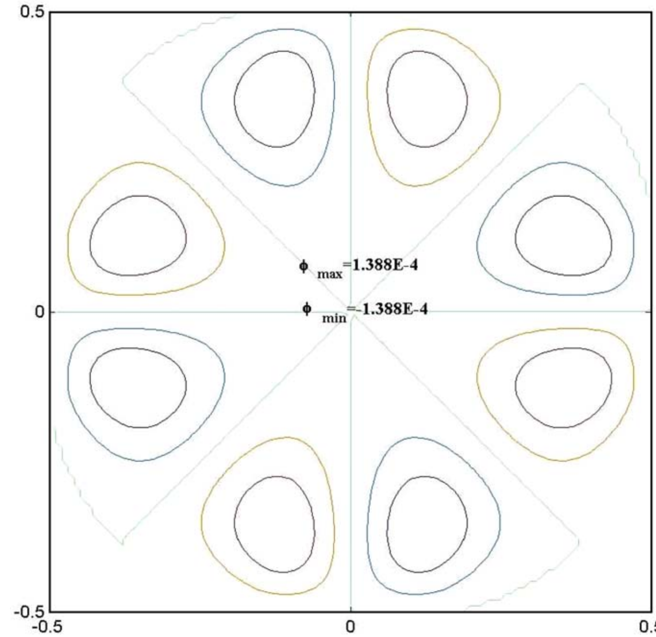

Fig. 6. Stream function contour plot ($n = 0.8$, $Re_g = 500$, $\psi_2^* = 0.01$, $r = 0.3$).

weaker vortices and in the limiting case for circular ducts, it approaches to zero.

References

[1] R.I. Tanner, Engineering Rheology, Oxford University, 2000.
[2] P. Twonsend, K. Walters, W.M. Waterhouse, Secondary flows in pipes of square cross-section and the measurement of second normal stress difference, Journal of Non-Newtonian Fluid Mechanics 1 (1976) 107–123.
[3] B. Gervang, P.S. Larsen, Secondary flows in straight ducts of rectangular cross-section, Journal of Non-Newtonian Fluid Mechanics 39 (1991) 217–237.
[4] S. Syrjala, Laminar flow of viscoelastic fluids in rectangular ducts with heat transfer: A finite element analysis, International Communications in Heat and Mass Transfer 25 (2) (1998) 191–204.
[5] M.F. Naccache, P.R. Souza Mendes, Heat transfer to non-Newtonian fluids in laminar flow through rectangular ducts, International Journal of Heat and Fluid Flow 17 (6) (1996) 613–620.
[6] S.X. Gao, J.P. Hartnett, Heat transfer behavior of Reiner–Rivlin fluids in rectangular ducts, International Journal of Heat and Mass Transfer 39 (6) (1996) 1317–1324.
[7] S.C. Xue, N. Phan-Thien, R.I. Tanner, Numerical study of secondary flows of viscoelastic fluid in straight pipes by an implicit finite volume method, Journal of Non-Newtonian Fluid Mechanics 59 (1995) 191–213.
[8] A.G. Dodson, P. Townsend, K. Walters, Non-Newtonian flow in pipes of non-circular cross-section, Computers and Fluids 2 (1974) 317.
[9] R.B. Bird, R.C. Armstrong, O. Hassager, Dynamics of Polymeric Liquids, vol. 1, John Wiley, New York, 1987.
[10] A. Bejan, Convection Heat Transfer, second ed., Wiley, New York, 1995.